Material Property Measurements of Micromechanical Polysilicon Beams

Raj K. Gupta, Peter M. Osterberg, and Stephen D. Senturia

Microsystems Technology Laboratories, Rm. 39-667
Massachusetts Institute of Technology, Cambridge, MA 02139 USA

October 1996

Copyright 1996 Society of Photo-Optical Instrumentation Engineers

This paper was published in Microlithography and Metrology in Micromachining II, and is made available as an electronic reprint (preprint) with permission of SPIE. Single print or electronic copies for personal use only are allowed. Systematic or multiple reproduction, or distribution to multiple locations through an electronic listserver or other electronic means, or duplication of any material in this paper for a fee or for commercial purposes is prohibited. By choosing to view or print this document, you agree to all the provisions of the copyright law protecting it.

Material property measurements of micromechanical polysilicon beams

Raj K. Gupta, Peter M. Osterberg, and Stephen D. Senturia

Microsystems Technology Laboratories, Rm. 39-667
Massachusetts Institute of Technology, Cambridge, MA 02139 USA

ABSTRACT

Fabrication- and measurement-induced stresses in surface micromachined structures are investigated by wafer-level probing of electrostatically actuated polysilicon test structures fabricated by the MUMPs process of MCNC. The test structures are based on M-Test, an electrostatic pull-in approach for monitoring process uniformity and reproducibility, and, when used in conjunction with suitable geometric data, for measuring material properties. The sensitivity of the pull-in technique reveals that the simple step of placing the die on a vacuum probe station can significantly affect the measured results. The presence of strain gradients in the polysilicon and compliant structural supports for the beams makes the modeling more complex than for ideal geometries, but with appropriate adjustments to the models, and with knowledge of the strain gradient obtained from cantilever tip deflection as a function of beam length, the technique enables a measurement of the elastic modulus and the fabrication-induced residual stress.

Keywords: MEMS mechanical property test structures, material property, elastic modulus, residual stress, polysilicon, modelling, surface micromachining, electrostatic pull-in.

INTRODUCTION

Methods for *in-situ* characterization of the elastic modulus or the residual stress from microelectromechanical systems (MEMS) have involved the measurement of resonant frequencies from beams [1-4] and comb-drives [5,6], the observation of stress relaxation in buckling or rotating structures [7-9], the capacitance-voltage measurement of a fixed-fixed beam bridge [10], the displacement measurement of a cantilever tip with the application of a known mechanical force [11], and the measurement of electrostatic pull-in test structures [1,2,7,12-15]. We have chosen the pull-in approach (M-Test) because of its ease of measurement, its adaptability to simple geometry test structures, and it tractability to well developed models.

MODELS FOR PULL-IN

M-Test [13] is based on measuring the dependence of pull-in voltage on a structural dimension, for example, the length of a fixed-fixed beam. The data are fit to closed-form expressions developed for ideal geometries (see Table 1), resulting in extracted parameters, B and S, which depend on a combination of material properties and geometric parameters. L represents the length of the cantilever beam or fixed-fixed beam, or the radius of the clamped circular diaphragm. The device thickness is t, and the electrostatic gap for a uniformly flat structure is g_o. Numerical constants used in Table 1 are shown in Table 2. Because B and S depend on high powers of the thickness and gap, accurate material property extraction from the values of B and S requires precise device metrology. [13-15]

The elastic modulus, $\tilde{E}$, and the residual stress, $\tilde{\sigma}$, contained in the Table 1 expressions for B and S are structure-dependent. For a circular diaphragm, $\tilde{E}$ is the plate modulus, given by $E/(1-\nu^2)$ for an isotropic material, where E is the Young's modulus and ν is the Poisson ratio, and $\tilde{\sigma}$ is equal to the residual biaxial stress σ_o. For cantilevers, $\tilde{\sigma}$ is zero, while for fixed-fixed beams, $\tilde{\sigma}$ is equal to the uniaxial stress $\sigma_o(1-\nu)$,

which is less than σ_o because of the Poisson contraction accompanying the release of stress perpendicular to the beam length. For both cantilevers and fixed-fixed beams, $\tilde{E}$ depends on the width of the beam [16]. For a slender beam having a width less than five times the thickness, $\tilde{E}$ approaches the Young's modulus, but for a wide beam having a width greater than five thicknesses, $\tilde{E}$ approaches the plate modulus.

In principle, by combining results from cantilevers, fixed-fixed beams, and circular diaphragms, it should be possible to extract all three quantities, E, ν , and σ_o. However, in practice, the requirement of placing sacrificial release etch holes in surface micromachined circular diaphragms modifies their structural behavior and requires modelling beyond the scope of this work. For this reason, we restrict our attention to relatively-wide cantilevers and fixed-fixed beams, from which we can determine the plate modulus and the residual uniaxial stress.

The compliant supports and a residual strain gradient $\partial\varepsilon_z/\partial z$ in the microstructures examined here complicate the analysis further than what was presented in [13]. The value of the strain gradient is obtained directly from the radius of curvature and is extracted from the length dependence of the cantilever tip deflection. The residual stress and the strain gradient introduce moments at the compliant supports of the fixed-fixed beams, causing deformation of the supports which, in turn, contribute to bowing of the structural beam. For this work, the two-dimensional fringing-field corrected finite-difference simulations of [13] were enhanced to take into account the compliant supports and curved beam geometries.

V_{PI}		
General	**Bending-Dominated (S -> 0)**	**Stress-Dominated (B -> 0)**
$\sqrt{\dfrac{\gamma_{1n} S}{\varepsilon_o L^2 D_n\left(\gamma_{2n}, k, L\right)\left[1+\gamma_{3n}\dfrac{g_o}{w}\right]}}$	$\sqrt{\dfrac{4\gamma_{1n} B}{\varepsilon_o L^4 \gamma_{2n}^2\left(1+\gamma_{3n}\dfrac{g_o}{w}\right)}}$	$\sqrt{\dfrac{\gamma_{1n} S}{\varepsilon_o L^2\left(1+\gamma_{3n}\dfrac{g_o}{w}\right)}}$

where,

$$D_n = 1 + \frac{2\left\{1-\cosh\left(\gamma_{2n} kL/2\right)\right\}}{\gamma_{2n} kL/2 \sinh\left(\gamma_{2n} kL/2\right)}, \quad k = \sqrt{\frac{12S}{B}}, \quad S = \tilde{\sigma} t g_o^3, \quad B = \tilde{E} t^3 g_o^3$$

n=1 (cantilevers), n=2 (fixed-fixed beams), n=3 (clamped circular diaphragms).

Table 1: Closed-form expressions for V_{PI}.

Numerical Constants	n=1 (cantilevers)	n=2 (fixed-fixed beams)	n=3 (circular diaphragm)
γ_{1n}	**0.07**	**2.79**	**1.55**
γ_{2n}	**1.00**	**0.97**	**1.65**
γ_{2n}	**0.42**	**0.42**	**0**

Table 2: Numerical constants for the closed-form expressions of Table 1.

EXPERIMENTAL RESULTS

Fixed-fixed beam and cantilever polysilicon test structures of 40 µm widths and of varying lengths were fabricated using the MUMPs process, with a nominal thickness of 2 µm and a free-space gap of 2 µm created from a sacrificial oxide, as shown in Figure 1. [17] A nitride layer of a nominal thickness $t_n = 0.5$ µm is used to electrically isolate the substrate from the anchor of the mechanical devices. During release, vertical stress gradients caused cantilevers to curl out of plane and fixed-fixed beams to bow due to the compliance of their raised supports. Net compressive stress in the polysilicon enhanced the bowing of fixed-fixed beams and caused significant pre-buckled bending.

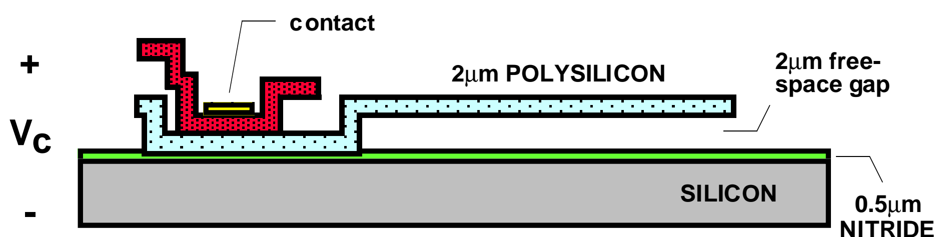

Figure 1: Simplified schematic of surface micromachined cantilever beam, showing the polysilicon thickness of 2 µm and a sacrificial spacer oxide layer (not shown) of 2 µm. Electrostatic voltage is applied between the polysilicon and the silicon substrate.

Deformation of the substrate by testing on a vacuum probe station introduced additional stress in fixed-fixed structures causing greater deformation. Its effect on the pull-in voltage characteristics is shown in Figure 2, where measurements were taken on a duplicate set of fixed-fixed beams with and without use of vacuum on the chuck. The substrate deformation increased the compressive stress in the polysilicon layer, decreasing the pull-in voltage of the smaller length beams. (See Figure 3) In beams 500 µm and longer, prebuckled bending dominated, bowing the beams significantly away from the substrate. As a result, the pull-in voltage discontinuously increased from that at 450 µm. At the length of 450 µm, the beam exhibited a tri-state region of operation. At voltages below pull-in, the beam which began bowed up, pulled-through to a second state in which it was bowed down and continued to deflect until it eventually pulled-in. In beams longer than 450 µm, the pull-through voltage was synonymous with the pull-in voltage, but at shorter lengths either the pull-through voltage was less than the pull-in voltage, or it was not observed.

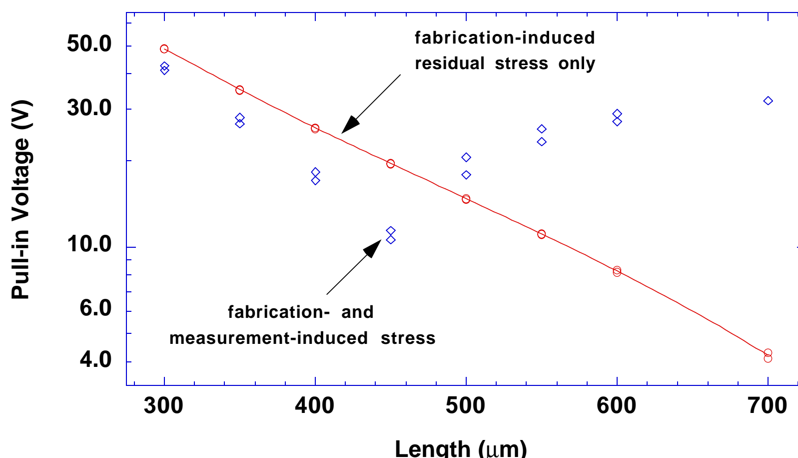

Figure 2: Pull-in measurements of fixed-fixed beams without vacuum (circles). Solid line fits this data to analytical model for ideal fixed-fixed beams. Also shown (diamonds) is pull-in with vacuum. See Figure 3 for a schematic interpretation.

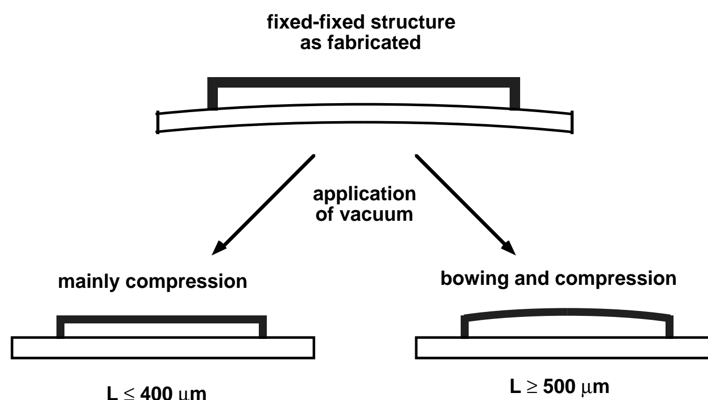

Figure 3: Schematic illustration of substrate deformation and effects of stress in fixed-fixed structures. L = 500 µm shows a tri-state behavior as explained in the text.

Surface contact profilometry was used for the metrology of the beams' thickness and free-space gap. In Figure 4, a Dektak™ measurement made by a 9 µg-force contact scanning across the length of a released cantilever revealed a polysilicon thickness of 2.10 µm and a free-space gap of 2.34 µm. A capacitance measurement across a polysilicon layer directly on top of the nitride layer and the silicon substrate yielded a dielectric thickness, t_n/ε_n, equal to 670 Å, where ε_n was the nitride permittivity. The electrostatic gap of a uniformly flat test structure was now calculated as the sum of the free-space gap and the dielectric thickness. The length of the devices were modified from the mask dimensions by the addition of the support compliance, which were modelled using I-DEAS™ FEM. It was found that approximately a 2 µm/support addition to the beam length was necessary to model the extra compliance. Using these dimensional values and based on the closed-form expressions in Table 1, we obtained $\tilde{E}$ = 149±10 GPa and a $\tilde{\sigma}$ = -3.5±0.5 MPa (compressive) from the no-vacuum pull-in data of the fixed-fixed beams in Figure 2. The error estimates are very approximate because we cannot bound the modelling errors at this time.

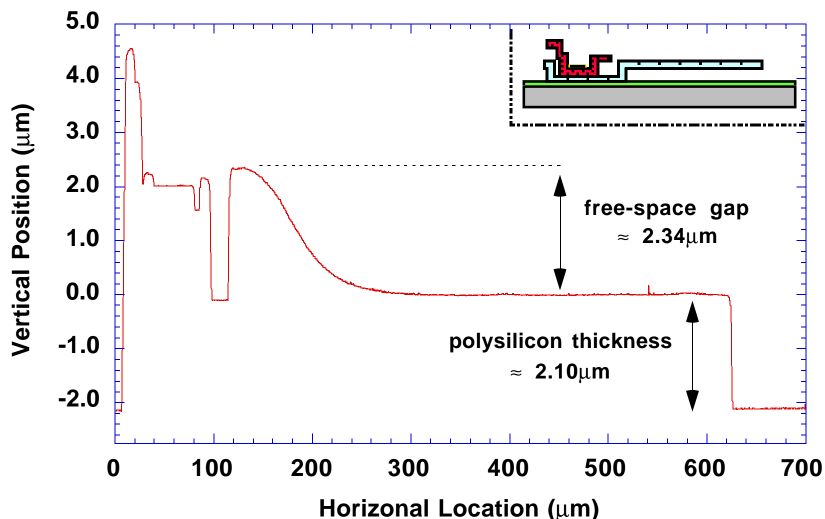

Figure 4: Dektak surface profilometry of a cantilever similar to the one shown in Figure 1 reveals the polysilicon and spacer oxide thickness. A 9µg force is applied at the tip of the scanning probe, pushing the cantilever down until it touches the nitride layer.

A 2D MATLAB™ finite-difference model [18] was developed for the pull-in of curled cantilevers, enabling the extraction of $\tilde{E}$, using the strain gradient as obtained by an optical tip deflection measurement. The fit in Figure 5 extracts an $\tilde{E}$ of 155±10 GPa using a $\partial\varepsilon_z/\partial z$ of $2.5\pm0.2\times10^{-5}$/µm. When multiplied by $\tilde{E}$, the strain gradient yields an approximate stress gradient of 4 MPa/µm within the unreleased and fixed-fixed polysilicon structures.

For reference and comparison, the experimental results from the various structures and measurement methods are summarized in Table 3.

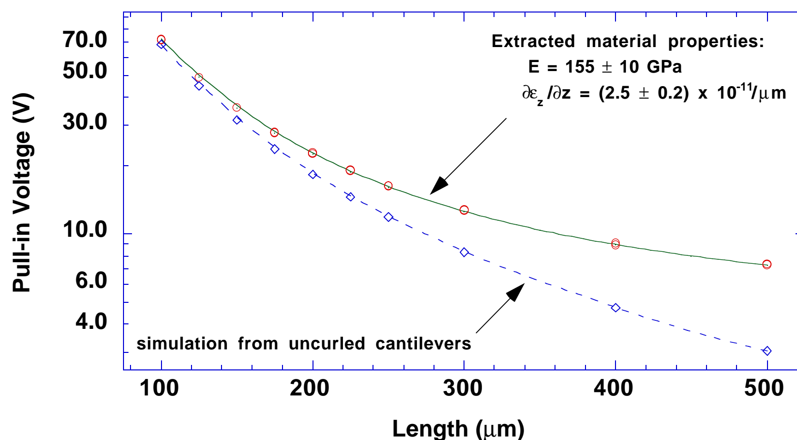

Figure 5: Measured pull-in data (circles) of curled cantilevers fit to a finite-difference model (solid line). Simulated pull-in data (diamonds) without cantilever curvature show the strong effect of curvature on pull-in.

CONCLUSIONS

We show that with careful electromechanical modelling and good data on structural geometries it is possible to extract the plate modulus and residual stress from the pull-in data of surface micromachined polysilicon beams, even in the presence of compliant supports and built-in strain gradients.

ACKNOWLEDGMENTS

This work was sponsored in part by the Semiconductor Research Corporation (Contract 95-SC-309) and by ARPA (Contracts J-FBI-92-196 and J-FBI-95-215).

	$\tilde{E}$	$\sigma_o(1-\nu)$	Strain Gradient, $\partial\varepsilon_z/\partial z$
Pull-in of Fixed-fixed beams:	149±10 GPa	-3.5±0.5 MPa	
Pull-in of Cantilevers:	155±10 GPa		
Optical tip deflection:			$2.5\pm0.2\times10^{-5}/\mu m$

Table 3: Summary of extracted material parameters.

References:

[1] K. E. Petersen, "Dynamic Micromechanics on Silicon: Techniques and Devices", *IEEE Trans. on Electron Devices*, **ED-25** (1978), pp. 1241-1250.

[2] H. A. C. Tilmans, "Micro-Mechanical Sensors using Encapsulated Built-in Resonant Strain Gauges", Ph.D. Thesis, MESA Research Institute of the University of Twente, Enschede, The Netherlands, 1993.

[3] H. Guckel, D. W. Burns, H. A. C. Tilmans, D. W. DeRoo, and C. R. Rutigliano, "Mechanical Properties of Fine Grained Polysilicon, The Repeatability Issue", *Proceedings of the IEEE Solid-State Sensors and Actuators Workshop*, Hilton Head, SC, June 1988, pp. 96-99.

[4] L. M. Zhang, D. Uttamchandani, and B. Culshaw, "Measurement of the Mechanical Properties of Silicon Resonators", *Sensors and Actuators A*, **29** (1991), pp. 79-84.

[5] W. C. Tang, "Electrostatic Comb Drive for Resonant Sensor and Actuator Applications", Ph.D. Thesis, University of California at Berkeley, 1990.

[6] M. Biebl, G. Brandl, and R. T. Howe, "Young's Modulus of *in-situ* Phosphorus-doped Polysilicon", *Proceedings of Transducers' 1995, Volume II*, Stockholm, June 1995, pp. 80-83.

[7] Q. Zou, Z. Li, and L. Liu, "New Methods for Measuring Mechanical Properties of Thin Films in Micromachining: Beam Pull-in Voltage (V_{PI}) Method and the Long Beam Deflection (LBD) Method", *Sensors and Actuators A*, **48**, (1995), pp. 137-143.

[8] H. Guckel, D. W. Burns, C. Visser, H. A. C. Tilmans, and D. DeRoo, "Fine-grained Polysilicon Films with Built-in Tensile Strain", *IEEE Trans. Electron Devices*, **35** (1988), pp. 800-801.

[9] B. P. van Drieënhuizen, J. F. L. Goosen, P. J. French, and R. F. Wolffenbuttel, "Comparison of Techniques for Measuring Both Compressive and Tensile Stress in Thin Films", *Sensors and Actuators A*, **37-38** (1993), pp. 756-765.

[10] S. Wang, S. Crary, and K. Najafi, "Electronic Determination of the Modulus of Elasticity and Intrinsic Stress of Thin Films using Capacitive Bridges", *MRS Symposium Proceedings*, **276** (1992), pp. 203-208.

[11] J. A. Schweitz, "Mechanical Characterization of Thin Films by Micromechanical Techniques", *MRS Bulletin*, July 1992, pp. 34-45.

[12] K. Najafi and K. Suzuki, "A Novel Technique and Structure for the Measurement of Intrinsic Stress and Young's Modulus of Thin Films", *Proceedings of MEMS 1989*, Salt Lake City, February 1989, pp. 96-97; K. Najafi and K. Suzuki, "Measurement of Fracture Stress, Young's Modulus, and Intrinsic Stress of Heavily Boron-Doped Silicon Microstructures", *Thin Solid Films*, **181** (1989), pp. 251-258.

[13] P. M. Osterberg and S. D. Senturia, "M-TEST: A Test Chip for MEMS Material Property Measurement using Electrostatically Actuated Test Structures", to be published in *JMEMS*.

[14] P. M. Osterberg, R. K. Gupta, J. R. Gilbert, and S. D. Senturia, "Quantitative Models for the Measurement of Residual Stress, Poisson's Ratio and Young's Modulus Using Electrostatic Pull-in of Beams and Diaphragms", *Proceedings of the 1994 Solid-State Sensor and Actuator Workshop*, Hilton Head, SC, June 1994, pp. 184-188.

[15] R. K. Gupta, C. H. Hsu, M. A. Schmidt and S. D. Senturia, "Monitoring Plasma Over-etching of Wafer-Bonded Microstructures", *Proceedings of Transducers' 1995, Volume 1*, Stockholm, June 1995, pp. 269-72.

[16] S. P. Timoshenko, "Theory of Plates and Shells," McGraw-Hill, 1987, pp. 4-6, 118, and 125.

[17] MUMPs 5 devices, courtesy of David Koester and Karen Markus.

[18] MATLAB™ scripts available by request from author, email: rajgupta@mtl.mit.edu.